Int Nano Lett (2017) 7:35–41
DOI 10.1007/s40089-017-0199-x

ORIGINAL ARTICLE

Kinetics adsorption study of the ethidium bromide by graphene oxide as adsorbent from aqueous matrices

M. Rajabi[1] · O. Moradi[2] · K. Zare[3,4]

Received: 12 September 2016 / Accepted: 11 January 2017 / Published online: 30 January 2017

Abstract In this study of ethidium bromide, adsorption from aqueous matrices by graphene oxide as adsorbent was investigated. Influencing parameters in the adsorption study included contact time, temperature, and pH. The optimum time was selected 17 min, and the best value of pH was determined at 8. All adsorption experiments were performed at 298 K temperature. The maximum wavelength of ethidium bromide was 475 nm. The Elovich, four types of the pseudo-second-order, the pseudo-first-order, and intra-particle diffusion kinetic adsorption models were used for kinetic study, and the results show that adsorption of ethidium bromide on graphene oxide surface best complied with type (I) of the pseudo-second-order kinetic model.

Keywords Kinetics · Adsorption · Ethidium bromide · Graphene oxide · Aqueous matrices

✉ M. Rajabi
mrajabi93@iau-arak.ac.ir; mostafa_moshavere@yahoo.com

O. Moradi
moradi.omid@gmail.com; o.moradi@shahryaiu.ac.ir

[1] Young Researchers and Elite Club, East Tehran Branch, Islamic Azad University, Tehran, Iran

[2] Department of Chemistry, Shahr-e-Qods Branch, Islamic Azad University, Tehran, Iran

[3] Department of Chemistry, Science and Research Branch, Islamic Azad University, Tehran, Iran

[4] Department of Chemistry, Shahid Beheshti University, Evin, Tehran, Iran

Introduction

Ethidium bromide (EtBr) is a potent mutagen and a toxic chemical [1]. It is also one intercalating common agent employed as a tag of fluorescent (nucleic acid stain) in laboratories of molecular biology for techniques, such as agarose gel electrophoresis [2]. Because the unique structure of EtBr resembles DNA, it can easily intercalate into DNA strand. Therefore, in the life science field, it is commonly used as nucleic acid fluorescent tag in various techniques.

Graphene is the thinnest known material, i.e., a sheet of carbon atoms could be arranged in hexagonal cells of only a single atom thick and yet be stronger than diamond [3]. Since it was experimentally isolated in 2004, it has been the object of intense theoretical and experimental research [4, 5]. Graphene oxide (GO) is similar to graphene, but presents oxygen-containing functional groups [5–8].

Recently, many studies have been done on the absorption process and have been compared with classical adsorbents, such as CNTs [9, 10], clay [11], activated carbon [12], graphene, and graphene derivatives, such as graphene oxide [13]. Graphene and graphene derivatives are more attractive recently because of their high selectivity, favorable physicochemical stability, and structural diversity. Extensive experiments have been conducted on the adsorption of organic or inorganic contaminants on graphene and graphene derivatives, such as Formaldehyde Molecule [14], Uranium(VI) [15], 1-naphthol [16], dyes [17], and adsorption of Pb(II) and Hg(II) [18]. Therefore, graphene and graphene derivatives might be good sorbents for the removal of contamination from water.

In this work, adsorption process was carried out for 17 min, 298 K, and pH 8 for removal ethidium bromide (EtBr) from aqueous matrices by graphene oxide (GO)

surface as adsorbent from aqueous matrices. Adsorption of ethidium bromide on graphene oxide surface was interpreted well by type (I) of the pseudo-second-order kinetic model.

Materials and methods

Materials

Ethidium bromide (EtBr) ($C_{21}H_{20}BrN_3$) used here was procured from Sigma-Aldrich Co. at 95% purity, and molecular weight was 394.31. NaOH and HCl were used to regulate the pH of the samples. The single-layer graphene oxide was prepared from Graphene Supermarket, (USA) with the following specifications: aqueous dispersion: concentration: 500 mg/L, 175 ml; composition: carbon (79%), oxygen (20%), flake size: 0.3–0.7 lm; thickness: 1 atomic layer–at least 80%; and brown color in all adsorption experiments as adsorbent. Specific surface area is determined to be 133 m^2/g (see Fig. 1).

Preparing GO surface

Graphene oxide was prepared from Graphene Supermarket, USA, and scanning electron microscopy of microstructures of GO surface used in this work is shown in Fig. 2.

Adsorption process study

Adsorption experiments were performed by adding 0.5 mg of graphene oxide (GO) surface as adsorbent into 20 mL of ethidium bromide (EtBr) solutions with known concentrations of 0.5 mg L^{-1}. The samples were collected, and the concentration of ethidium bromide in the aqueous matrices was determined after a specified period of time at 2, 5, 8, 11, 14, 17, and 20 min by applying the spectrophotometer of UV–VIS (Thermo Electron Corporation, Aquamate) at 475 nm, respectively. Thereupon, to study adsorption

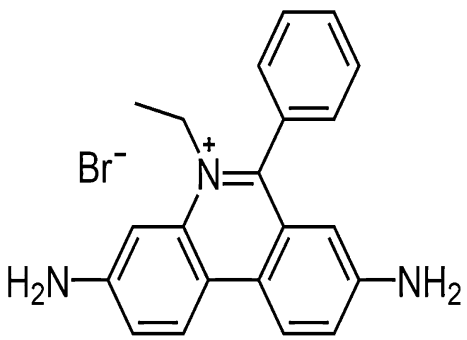

Fig. 1 Structure of ethidium bromide (EtBr)

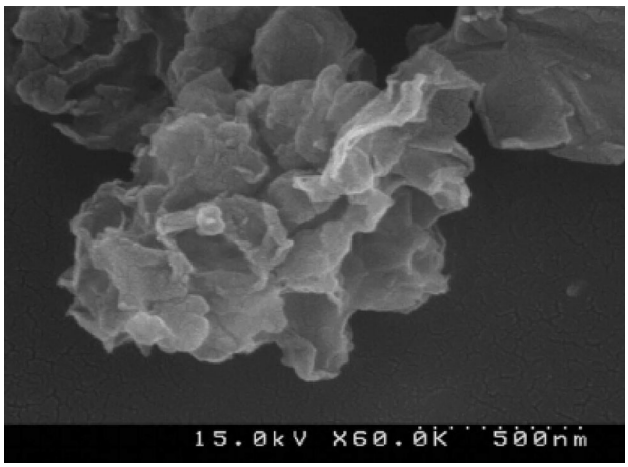

Fig. 2 SEM image of graphene oxide surface prepared from graphene Supermarket, (USA)

kinetic parameter (q_t), in mg/g, for ethidium bromide at time t Eq. (1) was used [19].

$$q_t = \left(\frac{C_0 - C_t}{W}\right) \times V, \tag{1}$$

where C_0 (mg L^{-1}) was the initial ethidium bromide concentration, C_t (mg L^{-1}) was the ethidium bromide concentration at time t, q_t (mg/g) was ethidium bromide adsorption capacity at time t, W (g) was adsorbent mass, and V (L) was the volume of ethidium bromide solution. Adsorption time curve for removal of ethidium bromide by GO as adsorbent is shown in Fig. 3.

The graphene oxide adsorption experiments were performed using the batch technique to determine the ethidium bromide adsorption capacity. After 17 min, no noticeable change was observed in the amount of absorption capacity of EtBr on the GO surface as adsorbent. Therefore, 17 min was selected as optimum time for removal of ethidium bromide by graphene oxide surface as adsorbent in all adsorption experiments.

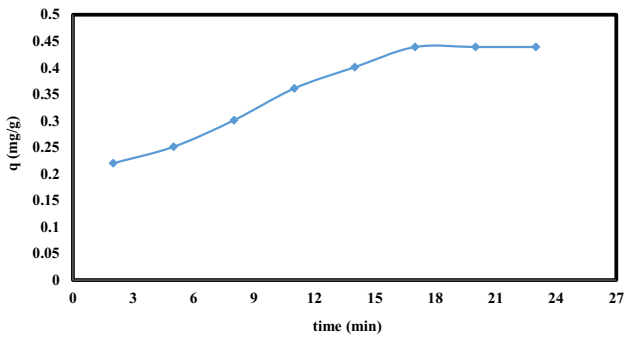

Fig. 3 Contact time effect of the adsorption ethidium bromide onto GO surface as adsorbent, initial concentration: 0.5 mg L^{-1}; dosage of adsorbent: 0.5 mg; temperature: 298 K and pH: 8

Result and discussion

GO characterizations

Graphene oxide surface was prepared from (Graphene Supermarket, USA), and scanning electron microscopy of microstructures of GO surface used here is presented in Fig. 2.

The effect of pH

Removal of ethidium bromide from solution by graphene oxide adsorbent was carried out at 17 min as optimum time at temperature 298 K, and to also for find the optimum value of pH, experiments of ethidium bromide adsorption onto graphene oxide surface were performed at different pH values from 2 to 10. With increasing the initial pH value of solution from 2 to 8, removal of EtBr by GO surface as adsorbent increased, and maximum amount of adsorption of (EtBr) on (GO) surface was at pH 8. Then, as shown in Fig. 4, with increasing initial pH value of solution from 8 to 10, (EtBr) removal by (GO) surface decreased.

Adsorption kinetics study

Adsorption kinetics experiments were conducted to obtain the resulting kinetic parameters and to investigate the effects of contact time. Figure 3 presents the variation in the adsorption of ethidium bromide by graphene oxide surface as adsorbent and as a function of contact time. It was noticed that after 17 min, no noticeable change was observed in the amount of absorption capacity of EtBr on the GO surface as adsorbent. Therefore, 17 min was selected as optimum time for removal of ethidium bromide by graphene oxide surface as adsorbent in all adsorption experiments. The adsorption kinetics of ethidium bromide was plotted using the Elovich, four types of the pseudo-second-order, the pseudo-first-order, and the intra-particle diffusion kinetic models.

The intra-particle diffusion kinetic model

For kinetic study, the constant rate for intra-particle diffusion is given by [20]:

$$Q_t = k_i(t)^{1/2} + C, \tag{2}$$

where 'Q_t' (mg/g) was the amount of ethidium bromide adsorbed on graphene oxide surface at different times t; C (mg/g) was a constant for the intra-particle diffusion model that gives an idea about the thickness of the boundary layer, and 'k' (mg/g $\text{min}^{1/2}$) was the intra-particle diffusion rate constant [21], determined by plotting. Figure 5 shows q_t versus plot $t^{1/2}$ q_t.

The Elovich kinetic model

At kinetic study the Elovich model is generally expressed as equation [22]:

$$\frac{\mathrm{d}q_t}{\mathrm{d}t} = \alpha \exp(-\beta q^2). \tag{3}$$

Elovich model liner form is expressed as Eq. (4) [22, 23]:

$$Q_t = \frac{1}{\beta}\ln(\alpha\beta) + \frac{1}{\beta}\ln t, \tag{4}$$

where 'β'(g/mg) was the extent of surface coverage, 'Q_t'(mg/g) was the amount of ethidium bromide adsorbed on graphene oxide surface at different times t, and 'α' (mg/g min) was the initial adsorption rate. The intercept and slope at the linear relationship of the plot of q_t versus ln t were used to determine α and β. Figure 6 shows the plot of q_t versus ln t.

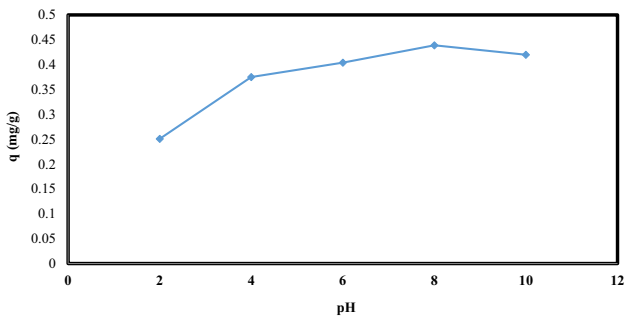

Fig. 4 Effect of pH on the adsorption ethidium bromide onto GO surface as adsorbent, initial concentration: 0.5 mg L^{-1}; dosage of adsorbent: 0.5 mg; temperature: 298 K and pH: 8

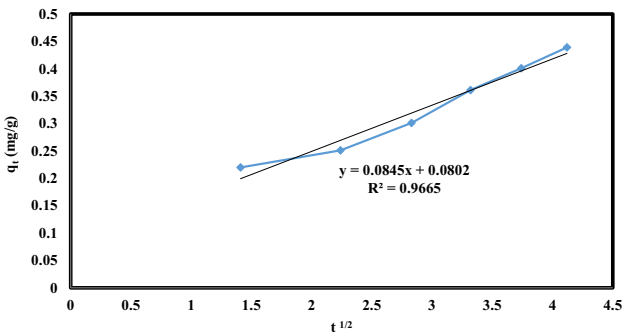

Fig. 5 Intra-particle diffusion adsorption kinetic of ethidium bromide on GO adsorbent. Conditions: initial concentration: 0.5 mg L^{-1}; dosage of adsorbent: 0.5 mg; temperature: 298 K and pH: 8

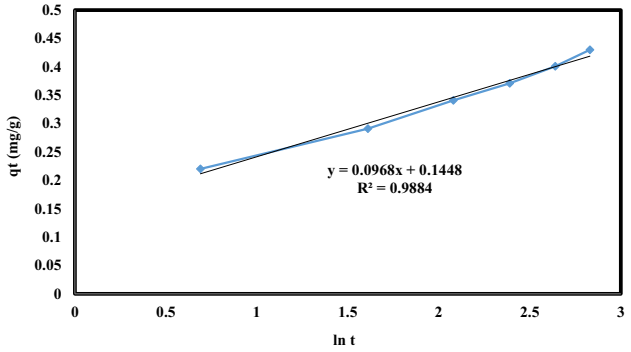

Fig. 6 Elovich adsorption kinetic of ethidium bromide on GO adsorbent. Conditions: initial concentration: 0.5 mg L^{-1}; dosage of adsorbent: 0.5 mg; temperature: 298 K and pH: 8

The pseudo-first-order kinetic model

In general, at kinetic studies, the pseudo-first-order kinetic model equation is expressed as [24–26]

$$\frac{dq_t}{dt} = k_1(q_e - q_t). \tag{5}$$

The integrated form of the pseudo-first-order kinetic model equation is as [27]

$$\log(q_e - q_t) = \log(q_e) - k_1 t, \tag{6}$$

where q_e and q_t were the amounts of ethidium bromide removed by graphene oxide adsorbent at equilibrium and t time, respectively. k_1 was the constant rate. By plotting values of log (q_e−q_t) versus t, q_e and k_1 can be determined from the intercept and slope, respectively. Figure 7 shows the plot of log (q_e−q_t) versus t.

The pseudo-second-order kinetic model

In general, at kinetic studies, the pseudo-second-order kinetic model equation is expressed as Eq. 7 presented by Ho in 1995 demonstrated how the rate depended on the adsorption equilibrium capacity [28, 29]:

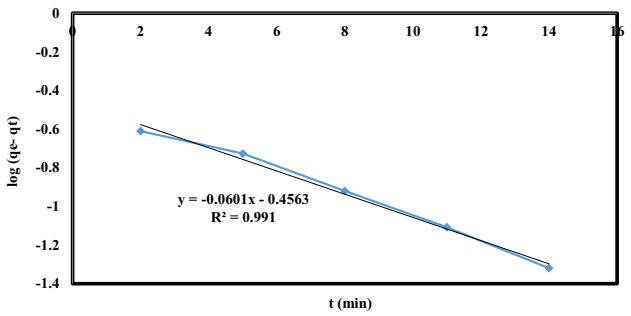

Fig. 7 Pseudo-first-order kinetic of ethidium bromide on GO adsorbent. Conditions: initial concentration: 0.5 mg L^{-1}; dosage of adsorbent: 0.5 mg; temperature: 298 K and pH: 8

$$\frac{dq_t}{dt} = k(q_e - q_t)^2. \tag{7}$$

An integrated pseudo-second-order rate can be obtained from Eq. (7) for the boundary conditions $q_t = 0$ to $q_t = q_t$ and $t = 0$ to $t = t$, which is given by [30]

$$\frac{1}{(q_e - q_t)} = \frac{1}{q_e} + kt. \tag{8}$$

By rearranging, Eq. (8) can take a linear form as

$$\frac{t}{q_t} = \frac{1}{k_2 q_{e^2}} + \frac{t}{q_e}, \tag{9}$$

where k_2 (g mg^{-1} min^{-1}) was the equilibrium rate constant of pseudo-second-order model; t (min) was the reaction time; q_e (mg g^{-1}) was the amount of adsorbate at equilibrium; and q_t (mg g^{-1}) was the amount of adsorbate at time t.

In this study, four types of linear forms of the pseudo-second-order kinetic model [31, 32] were used. Figures 8, 9, 10, 11 show the plots of four types of linear forms of the pseudo-second-order kinetic model.

The Chi-square statistic (χ^2) was used to evaluate the fitness of kinetic equations to the experimental data [13]. Chi-square statistic can be defined as

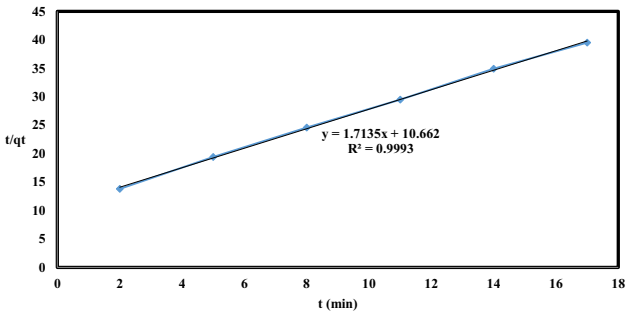

Fig. 8 Type 1 of pseudo-second-order kinetic of ethidium bromide on GO adsorbent. Conditions: initial concentration: 0.5 mg L^{-1}; dosage of adsorbent: 0.5 mg; temperature: 298 K and pH: 8

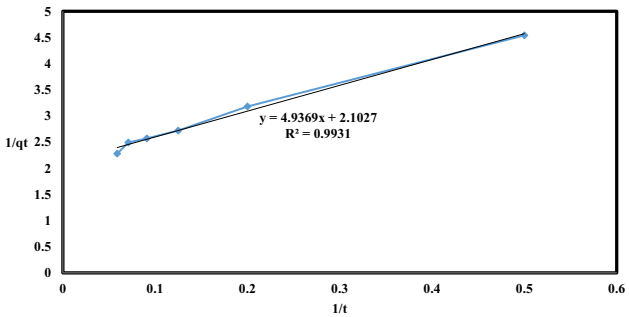

Fig. 9 Type 2 of pseudo-second-order kinetic of ethidium bromide on GO adsorbent. Conditions: initial concentration: 0.5 mg L^{-1}; dosage of adsorbent: 0.5 mg; temperature: 298 K and pH: 8

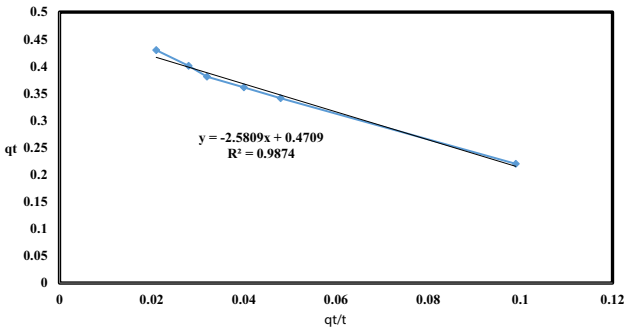

Fig. 10 Type 3 of pseudo-second-order kinetic of ethidium bromide on GO adsorbent. Conditions: initial concentration: 0.5 mg L^{-1}; dosage of adsorbent: 0.5 mg; temperature: 298 K and pH: 8

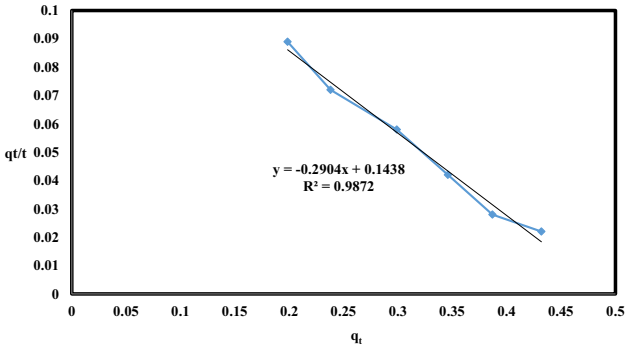

Fig. 11 Type 4 of pseudo-second-order kinetic of ethidium bromide on GO adsorbent. Conditions: initial concentration: 0.5 mg L^{-1}; dosage of adsorbent: 0.5 mg; temperature: 298 K and pH: 8

$$\chi^2 = \sum_i^N \frac{\left(q_{e,exp} - q_{e,cal}\right)^2}{q_{e,cal}}. \quad (10)$$

χ^2 will be a small number if the data from the experimental data are similar to the model, and χ^2 will be a large number if they are different. N is the number of observations in the experimental data, and the subscripts "calc" and "exp" show the calculated and experimental values, respectively.

According to the results of kinetic study listed in Tables 1 and 2, removal of ethidium bromide (EtBr) by graphene oxide (GO) surface as adsorbent from solution was well interpreted by pseudo-second-order kinetic model the type (I) because of low value of the Chi-square statistic (χ^2) and high value of the correlation coefficients (r^2).

Conclusions

In summary, adsorption capacity of ethidium bromide (EtBr) on graphene oxide (GO) surface as solution adsorbent was investigated. To remove ethidium bromide by graphene oxide adsorbent, 17 min was selected as optimum time as after 17 min, no noticeable change was observed in the amount of absorption capacity of EtBr on the GO surface. The results of pH effect showed that high amount of adsorption capacity of (EtBr) on (GO) surface was at pH 8; therefore, solution pH was fixed at pH 8. All adsorption experiments were performed at temperature 298 K. For kinetic study and to test adsorption experimental data the Elovich, the pseudo-first-order, the intra-particle diffusion, and the pseudo-second-order kinetic models were used. The results of kinetic study showed that adsorption of ethidium bromide on graphene oxide surface was well

Table 1 Pseudo-first-order, Elovich and intra-particle diffusion kinetic parameters for adsorption ethidium bromide on GO adsorbent

Model	Equation	Parameters	EtBr
Pseudo-first-order	$\log(q_e - q_t) = \log(q_e) - k_1 t$	q (mg/g)	0.350
		k_1 (1/min)	0.060
		r^2	0.991
		χ^2	4.99
Elovich	$q_t = \frac{1}{\beta}\ln \alpha\beta + \frac{1}{\beta}\ln t$	α	0.100
		β	10.42
		r^2	0.988
		χ^2	5.14
Intra-particle diffusion	$q_t = k_i t^{0.5} + C$	C	0.080
		k_i (1/min)	0.084
		r^2	0.966
		χ^2	6.71

Conditions: initial concentration: 0.5 mg L^{-1}; dosage of adsorbent: 0.5 mg; temperature: 298 K and pH: 8

Table 2 Four types of the pseudo-second-order kinetic of ethidium bromide on GO adsorbent

Type	Linear form	Plot	Parameters	EtBr
			q_e	0.584
Type (I)	$\frac{t}{q_t} = \frac{1}{kq_e^2} + \frac{1}{q_e}t$	t/q_t vs. t	k_{21}	0.275
			r^2	0.999
			χ^2	2.01
Type (II)	$\frac{1}{q_t} = \left(\frac{1}{kq_e^2}\right)\frac{1}{t} + \frac{1}{q_e}$	$1/q_t$ vs. $1/t$	q_e	0.476
			k_{22}	0.894
			r^2	0.993
			χ^2	8.41
			q_e	0.470
Type (III)	$q_t = q_e - \left(\frac{1}{kq_e}\right)\frac{q_t}{t}$	q_t vs. q_t/t	k_{23}	0.825
			r^2	0.987
			χ^2	7.70
			q_e	0.290
Type (IV)	$\frac{q_t}{t} = kq_e^2 - q_e q_t$	q_t/t vs. q_t	k_{24}	1.700
			r^2	0.987
			χ^2	7.26

Conditions: initial concentration: 0.5 mg L^{-1}; dosage of adsorbent: 0.5 mg; temperature: 298 K and pH: 8

interpreted by type (I) of the pseudo-second-order kinetic model because of the low value of the Chi-square statistic (χ^2) and high value of the correlation coefficients (r^2).

Acknowledgements The authors would like to thank the Young Researchers and Elite club, East Tehran Branch, Islamic Azad University for their financial support.

References

1. Lunn, G., Sansone, E.B.: Ethidium bromide: destruction and decontamination of solutions. Anal Biochem **162**, 453–458 (1987)
2. Stevenson, P., Sones, K.R., Gicheru, M.M., Mwangi, E.K.: Comparison of isometamidium chloride and homidium bromide as prophylactic drugs for trypanosomiasis in cattle at Nguruman, Kenya. Acta Trop **59**, 257–258 (1995)
3. Najafi, F., Rajabi, M.: Thermal gravity analysis for the study of stability of graphene oxide–glycine nanocomposites. Int Nano Lett **5**, 187–190 (2015)
4. Neto, A.H.C., Guinea, F., Peres, N.M.R., Novoselov, K.S., Geim, A.K.: The electronic properties of graphene. Rev Mod Phys **81**, 109 (2009)
5. Yari, M., Norouzi, M., Mahvi, A.H., Rajabi, M., Yari, A., Moradi, O., Tyagi, I., Gupta, V.K.: Removal of Pb(II) ion from aqueous solution by graphene oxide and functionalized graphene oxide-thiol: effect of cysteamine concentration on the bonding constant. Desalin Water Treat **57**(24), 11195–11210 (2016)
6. Choi, W., Lahiri, I., Seelaboyina, R., Kang, Y.S.: Synthesis of graphene and its applications: a review. Crit Rev Solid State Mater Sci **35**, 52–71 (2010)
7. Najafi, F., Moradi, O., Rajabi, M., Asif, M., Tyagi, I., Agarwal, S., Gupta, V.K.: Thermodynamics of the adsorption of nickel ions from aqueous phase using graphene oxide and glycine functionalized graphene oxide. J Mol Liq **208**, 106–113 (2015)
8. Dreyer, D.R., Park, S., Bielawski, C., Ruof, R.S.: The chemistry of graphene oxide. Chem Soc Rev **39**, 228–240 (2010)
9. Rajabi, M., Moradi, O., Mazlomifar, A.: Adsorption of methyl orange dye from water solutions by carboxylate group functionalized multi-walled carbon nanotubes. Int J Nano Dimens **6**(3), 227–240 (2015)
10. Robati, D., Bagheriyan, S., Rajabi, M.: Raman spectroscopy and TGA studies for the synthesis of multiwalled carbon nanotube-functionalized thiol (MWCNT-SH) nanocomposites: study of effect of concentration. Int Nano Lett **5**, 179–182 (2015)
11. Sedaghat, S.: Synthesis of clay–CNTs nanocomposite. J Nanostruct Chem **3**, 24 (2013)
12. Demiral, H., Güngör, C.: Adsorption of copper(II) from aqueous solutions on activated carbon prepared from grape bagasse. J Clean Prod **124**, 103–113 (2016)
13. Robati, D., Mirza, B., Rajabi, M., Moradi, O., Tyagi, I., Agarwal, S., Gupta, V.K.: Removal of hazardous dyes-BR 12 and methyl orange using graphene oxide as an adsorbent from aqueous phase. Chem Eng J **284**, 687–697 (2016)
14. Chi, M., Zhao, Y.: Adsorption of formaldehyde molecule on the intrinsic and Al-doped graphene: a first principle study. Comput Mater Sci **46**, 1085–1090 (2009)
15. Li, Z., Chen, F., Yuan, L., Liu, Y., Zhao, Y., Chai, Z., Shi, W.: Uranium(VI) adsorption on graphene oxide nanosheets from aqueous solutions. Chem Eng J **210**, 539–546 (2012)
16. Zhao, G., Li, J., Wang, X.: Kinetic and thermodynamic study of 1-naphthol adsorption from aqueous solution to sulfonated graphene nanosheets. Chem Eng J **173**, 185–190 (2011)
17. Fan, L., Luo, C., Sun, M., Qiu, H., Li, X.: Synthesis of magnetic-cyclodextrin–chitosan/graphene oxide as nanoadsorbent and its application in dye adsorption and removal. Colloids Surf B **103**, 601–607 (2013)
18. Zhang, Y., Yan, L., Xu, W., Guo, X., Cui, L., Gao, L., Wei, Q., Du, B.: Adsorption of Pb(II) and Hg(II) from aqueous solution using magnetic $CoFe_2O_4$-reduced graphene oxide. J Mol Liq **191**, 177–182 (2014)
19. Kim, H., Kang, S.O., Park, S., Park, H.S.: Adsorption isotherms and kinetics of cationic and anionic dyes on three-dimensional reduced graphene oxide macrostructure. J Ind Eng Chem **21**, 1191–1196 (2015)
20. Mishra, A.K., Ramaprabhu, S.: Functionalized graphene sheets for arsenic removal and desalination of sea water. Desalination **282**, 39–45 (2011)
21. Rajabi, M., Mirza, B., Mahanpoor, K., Mirjalili, M., Najafi, F., Moradi, O., Sadegh, H., Shahryari-ghoshekandi, R., Asif, M., Tyagi, I., Agarwalk, S., Gupta, V.K.: Adsorption of malachite green from aqueous solution by carboxylate group functionalized multi-walled carbon nanotubes: determination of equilibrium and kinetics parameters. J Ind Eng Chem **34**, 130–138 (2016)
22. Açıkyıldız, M., Gürses, A., Güneş, K., Yalvaç, D.: A comparative examination of the adsorption mechanism of an anionic textile dye (RBY 3GL) onto the powdered activated carbon (PAC) using various the isotherm models and kinetics equations with linear and non-linear methods. Appl Surf Sci **354**, 279–284 (2015)
23. Robati, D., Bagheriyan, S., Rajabi, M., Moradi, O., Peyghan, A.A.: Effect of electrostatic interaction on the methylene blue and

methyl orange adsorption by the pristine and functionalized carbon nanotubes. Phys E **83**, 1–6 (2016)
24. Alia, R.M., Hamad, H.A., Hussein, M.M., Malash, G.F.: Potential of using green adsorbent of heavy metal removal from aqueous solutions: adsorption kinetics, isotherm, thermodynamic, mechanism and economic analysis. Ecol Eng **91**, 317–332 (2016)
25. Yari, M., Rajabi, M., Moradi, O., Yari, A., Asif, M., Agarwal, S., Gupta, V.K.: Kinetics of the adsorption of Pb(II) ions from aqueous solutions by graphene oxide and thiol functionalized graphene oxide. J Mol Liq **209**, 50–57 (2015)
26. Fu, J., Chen, Z., Wang, M., Liu, S., Zhang, J., Zhang, J., Han, R., Xu, Q.: Adsorption of methylene blue by a high-efficiency adsorbent (polydopamine microspheres): kinetics, isotherm, thermodynamics and mechanism analysis. Chem Eng J **259**, 53–61 (2015)
27. An, C., Yang, S., Huang, G., Zhao, S., Zhang, P., Yao, Y.: Removal of sulfonated humic acid from aqueous phase by modified coal fly ash waste: Equilibrium and kinetic adsorption studies. Fuel **165**, 264–271 (2016)
28. Lee, J.J.: Equilibrium, kinetic and thermodynamic parameter studies on adsorption of acid yellow 14 using activated carbon. Korean Chem Eng Res **54**(2), 255–261 (2016)
29. Wongrueng, A., Sookwong, B., Rakruam, P., Wattanachira, S.: Kinetic adsorption of fluoride from an aqueous solution onto a dolomite sorbent. Eng J **20**(3), 1–9 (2016)
30. Koçer, O., Acemioğlu, B.: Adsorption of Basic green 4 from aqueous solution by olive pomace and commercial activated carbon: process design, isotherm, kinetic and thermodynamic studies. Desal W Treat **57**(35), 16653–16669 (2016)
31. Al-Jabari, M.: Kinetic models for adsorption on mineral particles comparison between Langmuir kinetics and mass transfer. Environ Technol Innov **6**, 27–37 (2016)
32. Hafeznezami, S., Zimmer-Faust, A.G., Dunne, A., Tran, T., Yang, C., Lam, J.R., Reynolds, M.D., Davis, J.A., Jay, J.A.: Adsorption and desorption of arsenate on sandy sediments from contaminated and uncontaminated saturated zones: Kinetic and equilibrium modeling. Environ Pollut Ser A **215**, 290–301 (2016)